# Local Symmetry Breaking by Impurities and Mode Splitting in Doped SmS

R. S. Fishman
*Solid State Division, Oak Ridge National Laboratory, Oak Ridge, Tennessee 37831-6032*

S. H. Liu
*Physics Department, University of California, San Diego, California 92093*
(Received 31 May 2002; published 26 November 2002)

We introduce the idea of local symmetry breaking by impurities to explain the recently observed splitting of the $J = 0 \rightarrow 1$ propagating excitation in doped $Sm_{1-x}Y_xS$. While preserving the global cubic symmetry of the crystal, Y impurities change the local crystal-field environment of each Sm ion from cubic to tetragonal, thereby splitting the $J = 1$ triplet into a $\mathbf{m}_i \cdot \mathbf{J} = 0$ level with energy $\Delta_1$ and a $\mathbf{m}_i \cdot \mathbf{J} = \pm 1$ doublet with energy $\Delta_2 > \Delta_1$. A model with a randomly oriented quantization axis $\mathbf{m}_i$ fits not only the observed mode frequencies but also their intensities, which strongly depends on the wave vector.

DOI: 10.1103/PhysRevLett.89.247203 PACS numbers: 75.10.Jm, 75.20.Ck, 75.25.+z

Materials with singlet ground states occupy an important place in condensed-matter physics [1–3] as testing grounds for ideas of magnetic coupling and spin-orbit interactions. One of the most important such materials is SmS, which contains a $J = 0$ ground state and a triply degenerate $J = 1$ excited state at energy $\Delta \approx 36.2$ meV, both constructed from the $S = 3$ and $L = 3$ $Sm^{2+}$ ion in a $4f^6$ configuration. Because of the magnetic coupling between different Sm ions, the $J = 0 \rightarrow 1$ excitation propagates through the crystal with a sizable dispersion, which was theoretically predicted by a number of authors [4–7] prior to its measurement by Shapiro *et al.* [8] over 25 years ago. One of the original motivations [9,10] for studying Sm monochalcogenides was to determine whether Sm is in a mixed $Sm^{2+}/Sm^{3+}$ valence state with an admixture of $4f^5 5d^1$. While there is no clear evidence for such an admixture in pure SmS, the $4f^5$ state can be produced by either pressure or by doping with Y, which applies an internal chemical pressure. External pressures above about 6.5 kbar [11] or Y concentrations above about 25% [12,13] transform the sample from a black semiconductor into a gold-colored metal. Because of the low carrier concentrations and strong Coulomb interactions, the mixed-valence state in the semiconductor probably involves the formation of a local bound state [3,14–16], which dissociates in the metallic phase.

Recent neutron-scattering measurements taken by Alekseev *et al.* [17] and plotted in Fig. 1 indicate that the $J = 0 \rightarrow 1$ propagating excitation in doped $Sm_{1-x}Y_xS$ splits into two for $x > 0$. There are two very surprising features of this data. First, the split modes remain well defined even for $x > 0$. Second, the mode intensities are strong functions of the wave vector. Whereas the low-frequency mode dominates at the zone center, it contains only about 1/3 of the total weight at the (111) zone boundary. This Letter demonstrates that Y impurities cause the observed mode splitting by breaking the local cubic symmetry about each Sm ion, thereby separating the $J = 1$ triplet into a $\mathbf{m}_i \cdot \mathbf{J} = 0$ level with energy $\Delta_1 < \Delta$ and a $\mathbf{m}_i \cdot \mathbf{J} = \pm 1$ doublet with energy $\Delta_2 > \Delta$. In contrast to the recent proposal [18] that the mode splitting in doped $Sm_{1-x}Y_xS$ is caused by its mixed valence, our simple model with randomly oriented quantization axis $\mathbf{m}_i$ can fit not only the mode frequencies but also their intensities.

The Hamiltonian of pure SmS can be written as $H = H_0 + H_{ex}$ where

$$H_0 = \Delta \sum_i \mathbf{L}_i \cdot \mathbf{S}_i, \tag{1}$$

$$H_{ex} = -\sum_{i,j} J_{ij} \mathbf{S}_i \cdot \mathbf{S}_j \tag{2}$$

are the spin-orbit energy and exchange interaction. The local $S = 3$ and $L = 3$ levels of the $4f^6$ ion are given by the spin-orbit energy $\Delta \mathbf{L} \cdot \mathbf{S} = \Delta J(J+1)/2 - 12\Delta$. Hence, the $J = 0$ ground state and the $J = 1$ excited states are separated by energy $\Delta$. Since $\Delta \approx 36$ meV

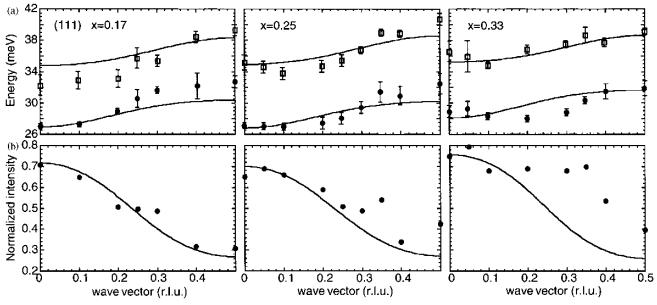


FIG. 1. The (a) measured mode frequencies and (b) relative intensity of the low-frequency mode for $Sm_{1-x}Y_xS$ with $x = 0.17$, 0.25, and 0.33 along the (111) direction at 17 K. Solid lines are two-parameter fits ($\Delta_1$ and $\Delta_2$) to both the frequencies and relative intensities using the exchange couplings of pure SmS.

  

and the exchange couplings are much smaller than $\Delta$, the $J = 2$ level with relative energy $3\Delta$ can be ignored below room temperature.

Applying the random-phase approximation (RPA) to the equations of motion for the Green's functions at $T = 0$ in the paramagnetic regime [19] yields the mode frequency [4,5]

$$\omega(\mathbf{q})^2 = \Delta^2 - 16J(\mathbf{q})\Delta. \tag{3}$$

Fits to the neutron-scattering data [8] indicate that at low temperatures $\Delta \approx 36.2$ meV, $J_1 \approx 0.043$ meV, and $J_2 \approx 0.025$ meV, where $J_1$ and $J_2$ are the nearest and next-nearest neighbor couplings on an fcc lattice. The third-nearest neighbor coupling $J_3$ was found to be much smaller than $J_2$.

Although they preserve the global cubic symmetry of the crystal, Y impurities break the local cubic symmetry around each Sm ion. For small Y concentrations, the local crystal-field environment around each $Sm^{2+}$ becomes tetragonal with quantization axis $\mathbf{m}_i$ pointing towards the nearest Y impurity. Whereas the $J = 0$ ground state $|G_1\rangle$ is unaffected, the $J = 1$ excited states split into a singly degenerate $\mathbf{m}_i \cdot \mathbf{J} = 0$ level $|G_2\rangle$ with energy $\Delta_1$ and doubly degenerate $\mathbf{m}_i \cdot \mathbf{J} = \pm 1$ levels $|D_\pm\rangle$ with energy $\Delta_2$. Our model treats the quantization axis $\mathbf{m}_i$ as a random vector but neglects local variations in the energies $\Delta_i$. Since the propagating $J = 0 \rightarrow 1$ excitations are not directly affected by the admixture of a $J = 5/2$, $4f^5$ state, we also ignore the mixed valence of the Sm ions. Despite these oversimplifications, our model explains all important features of the data, even in the metallic state with $x = 0.25$ and 0.33.

To obtain the mode frequencies at $T = 0$, we evaluate the retarded Green's function,

$$G_{ij}^{\alpha\beta}(\omega) = -i \int_0^\infty dt e^{i\omega t} \langle [S_{i\alpha}(t), S_{j\beta}(0)] \rangle. \tag{4}$$

This calculation is performed in two steps: First, we obtain the local Green's functions $\underline{G}_{ij}^{(0)}(\omega) = \delta_{ij}\underline{G}_i^{(0)}(\omega)$ with $J_{ij} = 0$ in the fixed, laboratory reference frame; then we use the RPA to obtain the full Green's functions.

Start by considering the local Green's functions in a local reference frame where $\mathbf{z}$ is parallel to $\mathbf{m}_i$. We shall need the nonzero matrix elements of $\mathbf{S}$ between the ground state and the three excited states: $\langle G_2|S_z|G_1\rangle = 2$ and $\langle D^+|S^+|G_1\rangle = -\langle D^-|S^-|G_1\rangle = -2\sqrt{2}$. Also bear in mind that the ground state $|G_1\rangle$ is nonmagnetic with $\langle G_1|\mathbf{S}|G_1\rangle = 0$. After inserting a complete set of states into Eq. (4), it is easy to show that the local Green's function in the local reference frame is given by $\bar{G}_{\alpha\beta}^{(0)}(\omega) = \delta_{\alpha\beta} g_\alpha(\omega)$, where $g_x(\omega) = g_y(\omega) \equiv g_2(\omega) = 8\Delta_2/d_2$, $g_z(\omega) \equiv g_1(\omega) = 8\Delta_1/d_1$, and $d_i = \omega^2 - \Delta_i^2$.

We must now relate the coordinate system of the fixed, laboratory reference frame to the coordinate system of the local reference frame at site $i$. The basis vectors of the local coordinate system at site $i$ are obtained by rotating the basis vectors $\mathbf{x}$, $\mathbf{y}$, and $\mathbf{z}$ of the laboratory coordinate system by angle $\theta_i$ about the unit vector $\mathbf{a}_i = \mathbf{x}\cos\phi_i + \mathbf{y}\sin\phi_i$. Then in terms of the spin $\mathbf{S}_i$ in the laboratory reference frame, the spin in the local reference frame is $\bar{\mathbf{S}}_i = \underline{U}_i \mathbf{S}_i$, where

$$\underline{U}_i = \begin{pmatrix} \cos^2\phi_i + \cos\theta_i \sin^2\phi_i & \frac{1}{2}(1 - \cos\theta_i)\sin 2\phi_i & -\sin\theta_i \sin\phi_i \\ \frac{1}{2}(1 - \cos\theta_i)\sin 2\phi_i & \sin^2\phi_i + \cos\theta_i \cos^2\phi_i & \sin\theta_i \cos\phi_i \\ \sin\theta_i \sin\phi_i & -\sin\theta_i \cos\phi_i & \cos\theta_i \end{pmatrix} \tag{5}$$

is a unitary matrix (its inverse is obtained by taking $\theta_i \rightarrow -\theta_i$). So the local Green's function in the laboratory reference frame is given by

$$\underline{G}_i^{(0)}(\omega) = \underline{U}_i^{-1} \bar{\underline{G}}^{(0)}(\omega) \underline{U}_i = g_2(\omega)\underline{I} + [g_1(\omega) - g_2(\omega)]\underline{E}_i, \tag{6}$$

where $\underline{I}$ is the unit matrix and

$$\underline{E}_i = \begin{pmatrix} \sin^2\theta_i \sin^2\phi_i & -\sin^2\theta_i \sin\phi_i \cos\phi_i & \sin\theta_i \cos\theta_i \sin\phi_i \\ -\sin^2\theta_i \cos\phi_i \sin\phi_i & \sin^2\theta_i \cos^2\phi_i & -\sin\theta_i \cos\theta_i \cos\phi_i \\ \sin\theta_i \cos\theta_i \sin\phi_i & -\sin\theta_i \cos\theta_i \cos\phi_i & \cos^2\theta_i \end{pmatrix} \tag{7}$$

depends on the angles of the local quantization axis at site $i$.

The full Green's function $\underline{G}_{ij}(\omega)$ is calculated by using a real-space version of the RPA which assumes that each site is visited just once. This is equivalent to a zeroth-order approximation [2,20] in $1/z$, where $z$ is the coordination number of the lattice. The resulting expression is

$$\underline{G}_{ij}(\omega) = \underline{G}_{ij}^{(0)}(\omega) - 2\sum_{l,m} \underline{G}_{il}^{(0)}(\omega) J(l - m) \underline{G}_{mj}(\omega), \tag{8}$$

where the local Green's function $\underline{G}_{ij}^{(0)}(\omega) = \delta_{ij}\underline{G}_i^{(0)}(\omega)$ is taken from Eq. (6).

There are three important cases of Eq. (8): in the absence of disorder with $\Delta_1 = \Delta_2$ (case I); in the presence of disorder with $\Delta_1 \neq \Delta_2$ and a random quantization axis (case II); and in the presence of a uniform strain field with $\Delta_1 \neq \Delta_2$ and a fixed quantization axis (case III). When $\Delta_1 = \Delta_2$ (case I), $g_1(\omega) = g_2(\omega) \equiv g(\omega)$ and $\underline{G}_i^{(0)}(\omega) = g(\omega)\underline{I}$. It follows that $\underline{G}_{ij}(\omega) = G_{ij}(\omega)\underline{I}$ is spin diagonal and satisfies the Fourier-transformed relation,

$$G(\mathbf{q}, \omega) = g(\omega) - 2g(\omega)J(\mathbf{q})G(\mathbf{q}, \omega). \tag{9}$$

We then recover the mode frequencies of Eq. (3) despite

the arbitrary orientation of the quantization axis at every site. So when the local $Sm^{2+}$ environment is cubic, the mode frequencies do not depend on the choice of local quantization axis.

For doped $Sm_{1-x}Y_xS$, the degeneracy of the $J = 1$ levels is broken by the Y impurities so that $\Delta_1 \neq \Delta_2$ and the quantization axis is random (case II). The RPA expression is then greatly simplified by averaging over the angles $\theta_i$ and $\phi_i$ of the quantization axis in the local Green's function. This procedure is tantamount to a virtual crystal approximation (VCA) [20] and leads to the simple results $\underline{E}_i \rightarrow \underline{I}/3$ and $\underline{G}^{(0)}(\omega) \rightarrow [g_1(\omega) + 2g_2(\omega)]\underline{I}/3$. Therefore, the full Green's function $\underline{G}_{ij}(\omega)$ is again spin diagonal and obeys

$$G(\mathbf{q}, \omega) = \tfrac{1}{3}[g_1(\omega) + 2g_2(\omega)] - \tfrac{2}{3}[g_1(\omega) + 2g_2(\omega)] \times J(\mathbf{q})G(\mathbf{q}, \omega). \quad (10)$$

A quadratic equation for $\omega^2$ finally yields the mode frequencies for case II:

$$d_1 d_2 + \frac{16}{3} J(\mathbf{q})(2\Delta_2 d_1 + \Delta_1 d_2) = 0, \quad (11)$$

which is satisfied by Eq. (3) when $\Delta_1 = \Delta_2$. Within the RPA and VCA, these modes are well defined even when $\Delta_1 \neq \Delta_2$. But a more sophisticated analysis would undoubtedly reveal that the random orientations of the quantization axis cause the modes to be damped.

For pure SmS, longitudinal fluctuations on site $i$ (corresponding to transitions from $|G_1\rangle$ to $|G_2\rangle$) remain longitudinal as they propagate through the lattice; similarly for transverse fluctuations (transitions from $|G_1\rangle$ to $|D^{\pm}\rangle$). In the random alloy, longitudinal or transverse fluctuations on one site obtain a mixed component when they propagate to a nearby site with a rotated quantization axis. This behavior is easier to see in the local reference frame, where the locally longitudinal and transverse fluctuations couple to one another when $J(\mathbf{q}) \neq 0$.

From Eq. (10), we obtain the neutron-scattering intensity,

$$S(\mathbf{q}, \omega)_{\alpha\beta} = -\delta_{\alpha\beta} \frac{8}{3\pi} \mathrm{Im}\left\{ \frac{2\Delta_2 d_1 + \Delta_1 d_2}{d_1 d_2 + 16J(\mathbf{q})(2\Delta_2 d_1 + \Delta_1 d_1)/3} \right\}_{\omega \rightarrow \omega + i\varepsilon}, \quad (12)$$

which is isotropic and reduces to the proper result when $\Delta_1 = \Delta_2$. At the (111) zone boundary, $J(\mathbf{q}) \approx -6J_2$ is very small. Hence, the modes at the zone boundary are almost local with frequencies $\omega_1 \approx \Delta_1$ and $\omega_2 \approx \Delta_2$. Because mode 2 is locally transverse and mode 1 is locally longitudinal, the ratio of their intensities at the zone boundary should be roughly 2 to 1. Experimentally, the high-frequency mode dominates near the zone boundary with relative weight $r_2 \approx 2/3$. It follows that $\Delta_2 > \Delta_1$ or that the $J = 1$, $\mathbf{m}_i \cdot \mathbf{J} = \pm 1$ doublet lies higher in energy than the $J = 1$, $\mathbf{m}_i \cdot \mathbf{J} = 0$ singlet. Away from the zone boundary, $J(\mathbf{q})$ becomes quite large and the mixing of the locally transverse and longitudinal fluctuations shifts the weight between the two modes.

Fits of this model to the measured mode frequencies *and* intensities along the (111) direction are plotted by the solid curves in Fig. 1, where the exchange couplings $J_1$ and $J_2$ are fixed by their values in pure SmS and $J_3$ is set to zero. Considering the simplicity of our model, these fits are quite good and describe all important features of the data. Results for the fitting parameters $\Delta_i$ are plotted in Fig. 2 and reveal that the weighted average $\bar{\Delta} = (2\Delta_2 + \Delta_1)/3$ is little changed by doping. This confirms our conjecture that the local symmetry around each $Sm^{2+}$ ion is tetragonal. The difference $\Delta_2 - \Delta_1$ between the two gaps begins to collapse at $x = 0.33$, which may arise from the change in the local, crystal-field environment from tetragonal to spherical as the number of Y impurities increases.

As already suggested, the shift in intensity between the low- and high-frequency modes results from the mixing of locally longitudinal and transverse fluctuations. If the quantization axis $\mathbf{m}_i = \mathbf{z}$ were the same at every site (case III), such as in a crystal with uniaxial strain along the $z$ axis, then $\underline{G}^{(0)}(\omega)$ would be spin diagonal with $G^{(0)}_{xx}(\omega) = G^{(0)}_{yy}(\omega) = g_2(\omega)$ and $G^{(0)}_{zz}(\omega) = g_1(\omega)$. It follows that $\underline{G}(\mathbf{q}, \omega)$ is likewise spin diagonal with $G_{xx}(\mathbf{q}, \omega) = G_{yy}(\mathbf{q}, \omega) \equiv A_2(\mathbf{q}, \omega)$ and $G_{zz}(\mathbf{q}, \omega) \equiv A_1(\mathbf{q}, \omega)$, where

$$A_i(\mathbf{q}, \omega) = g_i(\omega) - 2g_i(\omega)J(\mathbf{q})A_i(\mathbf{q}, \omega). \quad (13)$$

Hence, the mode frequencies $\omega_i$ $(i = 1, 2)$ in case III satisfy

$$\omega_i^2 = \Delta_i^2 - 16J(\mathbf{q})\Delta_i, \quad (14)$$

which agrees with the result of Hsieh [6]. While such a model can easily fit the observed mode frequencies, the

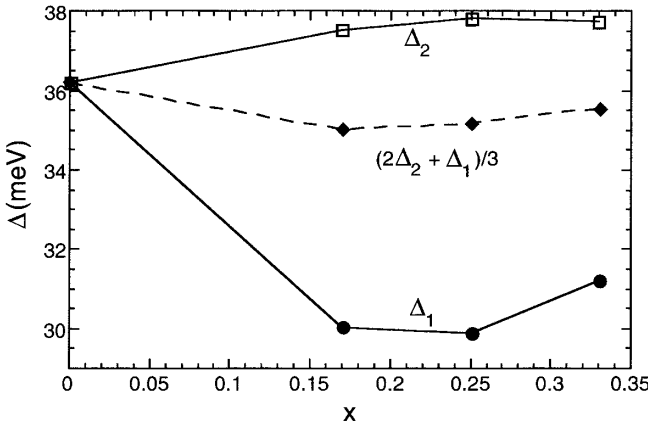


FIG. 2. The fitting results for $\Delta_1$ and $\Delta_2$ from the data in Fig. 1. Also plotted is the weighted average of the two gaps.

high-frequency, transverse mode would always have roughly twice the weight as the low-frequency, longitudinal mode so that $r_1 \approx 1/3$ for all $\mathbf{q}$. Thus, the observed shift in mode intensities with wave vector implies that the quantization axis must vary from site to site.

Although our simple model explains all important features of the neutron-scattering data, it is far from complete. A more sophisticated model for the mode splitting in $Sm_{1-x}Y_xS$ would account for the short-range correlations in the orientations of the quantization axis and for the local variations in the energy gaps $\Delta_1$ and $\Delta_2$, which may be expected to depend on the concentration of nearby Y impurities. However, the most serious shortcoming of our model is that it neglects the mixed valence of the Sm ions, which may be responsible for the unusual behavior of other singlet ground-state materials [3,14–16].

Indeed, a very recent paper [18] argues that the mode splitting in the $x = 0.17$ sample of $Sm_{1-x}Y_xS$ is caused by its mixed- valence. To explain the neutron-scattering intensities, the authors of Ref. [18] introduce an arbitrary $q$-dependent hybridization between two modes with frequencies given by Eq. (14). If the mode splitting were caused by the mixed-valence of doped $Sm_{1-x}Y_xS$, then the mode frequencies and intensities should display some signature of the semiconductor-to-metal transition at $x \approx 0.25$. The mixed-valence also fails to explain the roughly 2 to 1 ratio of the mode intensities at the zone boundary for each $x$. By contrast, local symmetry breaking provides a natural explanation for both the mode splitting and the neutron-scattering intensities for all Y concentrations.

A simple experiment to test the predictions of this paper would subject a doped sample of $Sm_{1-x}Y_xS$ to uniaxial strain (say in the $z$ direction). As the tetragonal distortion along the $z$ direction dominates over the random distortions produced by the Y impurities, the local quantization axis at every site will rotate towards $\mathbf{z}$ and the modes will become purely transverse or longitudinal with respect to $\mathbf{z}$, as in case III discussed above. Consequently, the relative intensity of the low-frequency mode will drop to $r_1 \approx 0.33$ across the Brillouin zone.

In summary, we have introduced the idea of local symmetry breaking to explain the mode splitting and neutron-scattering intensities in doped $Sm_{1-x}Y_xS$. Although quite simple, this model successfully describes all important features of the data. Local symmetry breaking by random impurities may also play an important role in many other systems.

It is a pleasure to acknowledge helpful conversations with Dr. Pavel Alekseev, Dr. Alexander Chernyshev, and Dr. Herb Mook. This research was sponsored by the U.S. Department of Energy under Contract No. DE-AC05-00OR22725 with Oak Ridge National Laboratory, managed by UT-Battelle, LLC.

[1] R. J. Birgeneau, J. Als-Nielsen, and E. Bucher, Phys. Rev. Lett. **27**, 1530 (1971).
[2] P. Bak, Phys. Rev. B **12**, 5203 (1975).
[3] J.-M. Mignot and P. A. Alekseev, Physica (Amsterdam) **215B**, 99 (1995).
[4] Y.-L. Wang and B. R. Cooper, Phys. Rev. **172**, 539 (1968).
[5] Y. Y. Hsieh and M. Blume, Phys. Rev. B **6**, 2684 (1972).
[6] Y. Y. Hsieh, Phys. Rev. B **8**, 3459 (1973).
[7] M. Blume and R. J. Birgeneau, J. Phys. C **7**, L282 (1974).
[8] S. M. Shapiro, R. J. Birgeneau, and E. Bucher, Phys. Rev. Lett. **34**, 470 (1975).
[9] R. J. Birgeneau, E. Bucher, L. W. Rupp, Jr., and W. M. Walsh, Jr., Phys. Rev. B **5**, 3412 (1972).
[10] M. Campagna, E. Bucher, G. K. Wertheim, and L. D. Longinotti, Phys. Rev. Lett. **33**, 165 (1974).
[11] A. Jayaraman, V. Narayanamurti, E. Bucher, and R. G. Maines, Phys. Rev. Lett. **25**, 1430 (1970).
[12] A. Jayaraman, E. Bucher, P. D. Dernier, and L. D. Longinotti, Phys. Rev. Lett. **31**, 700 (1973).
[13] T. Penney and F. Holtzberg, Phys. Rev. Lett. **34**, 322 (1975).
[14] T. Kasuya, Europhys. Lett. **26**, 277 (1994); **26**, 283 (1994).
[15] K. A. Kikoin and A. S. Mishchenko, J. Phys. Condens. Matter **7**, 307 (1995).
[16] J. C. Cooley, M. C. Aronson, Z. Fisk, and P. C. Canfield, Phys. Rev. Lett. **74**, 1629 (1995).
[17] P. A. Alekseev, V. N. Lazukov, J.-M. Mignot, and I. P. Sadikov, Physica (Amsterdam) **281B&282B**, 34 (2000); P. A. Alekseev, J.-M. Mignot, U. Staub, A. Ochiai, A. V. Golubkov, M. Braden, R. I. Bewley, E. V. Nefeodova, I. P. Sadikov, E. S. Clementyev, V. N. Lazukov, and K. S. Nemkovski, Physica (Amsterdam) **312B&313B**, 333 (2002).
[18] P. A. Alekseev, J.-M. Mignot, A. Ochiai, E. V. Nefeodova, I. P. Sadikov, E. S. Clementyev, V. N. Lazukov, M. Braden, and K. S. Nemkovski, Phys. Rev. B **65**, 153201 (2002).
[19] The Hamiltonian $H = H_0 + H_{ex}$ admits a ferromagnetic solution when the exchange coupling is sufficiently large. A ferromagnetic instability can be obtained from the condition that one of the mode frequencies vanishes at $\mathbf{q} = 0$. For SmS and its alloys, the exchange coupling is far too weak to stabilize a ferromagnetic ground state. In principle, however, the magnetic solution for a system with random quantization axis would be a spin glass.
[20] J. Jensen and A. R. Mackintosh, *Rare Earth Magnetism: Structures and Excitations* (Oxford University Press, Oxford, 1991).